scientific reports

Check for updates

OPEN

Optimization of power grid material warehousing and supply chain distribution path planning based on improved PSO algorithm

Junping Ge[1]✉, Tao Wang[2], Kairui Hu[1], Jianguo Wang[1], Jianchao Wu[1], Jing Wang[1] & Jianfeng Wu[1]

With the deepening of smart grid construction, the complexity of power grid material warehousing and emergency distribution continues to increase, which puts higher demands on efficient and scalable optimization models. In response to the problems of insufficient search efficiency and weak adaptability to dynamic disaster scenarios in traditional methods, this study proposes an optimization model that integrates a multi-strategy collaborative adaptive chaotic particle swarm optimization algorithm and an improved imperialist competitive algorithm. The experiment is conducted based on multiple types of emergency scenarios, and the results show that the accuracy of material classification of the model is as high as 98.73%, and the delivery time is shortened from 6.78 h to 4.56 h in earthquake scenarios. In the solution of the supply chain distribution path, the single iteration calculation is only 0.45s, which combines stability and efficiency. This model improves the search diversity of inventory parameter optimization by introducing multi-strategy chaotic disturbances and adaptive inertia weights, and combines fishbone warehouse layout to enhance picking efficiency. In the path planning stage, research is conducted to enhance the adaptability of algorithms to complex constraints and dynamic environments through immune penalty correction mechanisms and pheromone adaptive balancing strategies. Research results denote that this model has significant advantages in multi-objective optimization, warehouse layout planning, and emergency logistics path scheduling. This study provides feasible technical solutions for smart grid material management and emergency distribution, as well as new methodological references for complex supply chain optimization research.

Keywords Warehouse optimization, Path planning, Particle swarm optimization algorithm, Imperialist competitive algorithm, Multi-objective optimization, Metaheuristics, Resilience logistics

With the acceleration of the construction of new power systems, the complexity and dynamism of power grid material management have significantly increased, and traditional warehousing and logistics models are facing multiple challenges[1]. The variety of material categories is complex, covering thousands of categories such as power transmission and transformation equipment, emergency repair tools, etc., leading to confusion in classification and low storage efficiency[2–4]. The demand for emergency response has surged, and the contradiction between high equipment repair time requirements and insufficient inventory dynamic allocation capabilities in disaster scenarios such as typhoons and earthquakes is prominent[5]. In addition, the supply chain collaboration is fragmented, resulting in a lack of real-time linkage between inventory status and distribution path planning, as well as significant errors in manual inventory counting, leading to high logistics costs[6–8]. In this context, studying the optimization of power grid material warehousing and supply chain distribution path planning not only helps to improve the operational management level of power grid enterprises, but also enhances the power grid's material guarantee capability in emergency situations. In terms of warehouse optimization, L. Peng et al. proposed a multi-warehouse joint replenishment and distribution algorithm based on trade credit to address the issue of multi-warehouse joint replenishment and distribution. The experiment showed that this method could reduce total costs and achieve joint management of multiple warehouses[9]. X. Hu et al. designed a nonlinear programming model based on system layout planning and utilized genetic algorithm optimization

[1]Jinhua Power Supply Company, State Grid Zhejiang Electric Power Co., Ltd., Jinhua 321000, China. [2]State Grid Zhejiang Electric Power Co., Ltd., Hangzhou 310007, China. ✉email: ejhgjp@126.com

method to solve the problem of unreasonable layout of e-commerce warehouses affecting logistics efficiency. The experiment showed that the optimization rate of this method was 39.25%, which can reduce handling costs and improve picking efficiency[10]. J. N. Das et al. proposed an interdependent Pareto ant colony optimization (ACO) model based on deep embedding clustering to address the optimization problems of warehouse allocation and carton configuration in e-commerce logistics. The experiment denoted that the model could provide optimal or non-dominated solutions in all cases, effectively balancing transportation costs and carton volume[11].

In terms of supply chain transportation path optimization, Y. Wang et al. designed a multi-objective mixed integer linear programming model based on geographic information system with epsilon constraints to solve the problem of hazardous chemical transportation path optimization. The experiment showed that the model could consider the influence of buildings and perform well[12]. X. Hu et al. designed a multi-objective path optimization model to address the coordination problem between government and enterprise goals in multimodal transportation path optimization. The model balanced government carbon reduction and enterprise cost control objectives, and introduced fuzzy demand to handle demand fluctuations. An improved sparrow search algorithm was applied to address the problem. The experiment indicated that the multi-objective path optimization model could significantly reduce carbon dioxide emissions while moderately increasing costs[13]. D. Mahat et al. proposed using ACO algorithm to solve the optimization problems of mechanical engineering supply chain and logistics. Experiment demonstrated that the ACO algorithm had significant effects in inventory management, transportation route optimization, and production scheduling, which can reduce inventory costs, optimize transportation routes, and improve production efficiency[14].

In other aspects, V. H. S. Pham et al. proposed a hybrid whale optimization algorithm (hGWOA) by combining whale optimization algorithm with grey wolf optimizer to optimize supply chain transportation routes. The results indicated that in scenarios involving scale and complexity, the supply chain network optimized by hGWOA outperformed other algorithms in optimizing delivery distance[15]. J. Qezelbash Chamak et al. proposed a branch cutting algorithm for fast mixed integer programming to quickly respond to the needs of disaster emergency scenarios. The results indicated that this method improved the efficiency of establishing response plans[16].

The specific scientific shortcomings of previous methods are as follows: (1) Traditional Particle Swarm Optimization (PSO) and variants rely on fixed or empirical parameters, making it difficult to adapt to dynamic environments and multi-objective coupled optimization; (2) In high-dimensional space, particles are prone to local optima and population diversity drops sharply; (3) Although Independent Component Analysis (ICA) and ACO improve convergence accuracy, they are difficult to deal with nonlinear coupling and multi constraint problems; Hybrid algorithms are mostly a combination of heuristic structures, lacking a unified optimization framework and convergence analysis; (4) Reinforcement learning is not combined with data-driven approaches, resulting in poor adaptability to dynamic scenarios; Pure data-driven methods have high training costs and unstable convergence.

The prior PSO improvements had the following limitations: (1) insufficient adaptive mechanisms, lack of dynamic scene adaptation in improvements such as inertia weighting, and difficulty in balancing global search and local convergence; (2) The mixed strategy lacks synergy, and multiple algorithms are simply stacked, which can easily lead to conflicts and slow convergence and poor stability; (3) The maintenance of diversity is weak, and initialization methods (such as anti initialization) are difficult to avoid population convergence during iterations; (4) Weak theoretical support, lack of convergence and stability analysis, and poor scenario universality.

The reasons for the poor performance of existing multi-objective or adaptive hybrid methods are as follows: Firstly, traditional multi-objective PSO algorithms and their variants often rely on fixed or empirically set parameters, which have poor adaptability to dynamic environments and multi-objective coupled optimization. Secondly, the lack of real-time data interaction makes it difficult to cope with dynamic constraints and changes in target priority. Therefore, it cannot achieve better results.

Existing research is mostly conducted under a single optimization objective or deterministic assumption, and insufficient consideration is given to uncertain factors such as dynamic demand fluctuations, path disturbances, and sudden situations under multi-objective coupling conditions, which limits the practical applicability of algorithms in complex supply chain scenarios. To improve the efficiency and adaptability of power grid material warehousing and supply chain distribution, a power grid material warehousing optimization method based on Multi-strategy Collaborative Adaptive Chaotic Particle Swarm Optimization (MSC-PSO) and a supply chain distribution path planning method based on Improved Imperialist Competitive Algorithm (IICA) were proposed, and the MSC-PSO-IICA model was formed. To address the high uncertainty and multi-constraint scheduling problem of power grid logistics in the event of emergencies, this study formalizes the research problem as a multi-objective stochastic optimization model, with optimization objectives including: (1) Based on existing heuristic scheduling models, factors such as demand fluctuations, path interruptions, and scheduling delays are modeled in the form of probability distributions, thus forming a formal description of multi-objective stochastic optimization. This breaks away from the previous modeling methods that relied on empirical weights and deterministic scenarios, and provides a mathematical foundation for emergency supply chain optimization. (2) The concept of "chaotic perturbation + adaptive inertial weight + immune selection" is theoretically abstracted as a verifiable evolutionary update strategy. By constructing the Lyapunov function, the probabilistic convergence condition is given, proving that the mechanism can maintain population diversity in high-dimensional constrained spaces and overcome the problems of local convergence and unstable results of the original algorithm. (3) On the basis of the original engineering design integrating PSO and ICA/ACO, a hierarchical complexity analysis of the search process is carried out, and the worst time complexity limits for the path planning stage and warehouse optimization stage are given. It is proved that compared with traditional hybrid swarm intelligence algorithms, the algorithm reduces computational costs and improves scalability

without sacrificing accuracy. (4) Construct a multi-objective optimization function that integrates path, cost, response through weighted decomposition and Pareto frontier screening methods.

Method and materials

Optimization method for power grid material warehousing based on MSC-PSO algorithm

In the construction and operation of the power grid, the management of power grid material warehousing and supply chain distribution are crucial for cost control and power supply guarantee[17,18]. However, traditional power grid material warehousing and supply chain distribution have many shortcomings, such as the coexistence of inventory backlog and shortage, unreasonable distribution path planning, resulting in high logistics costs, low resource utilization, and slow emergency response[19]. To cope with the complexity of the power grid material storage system, the MSC-PSO algorithm is proposed. The MSC-PSO algorithm can effectively balance the global search capability and local convergence speed of the algorithm by adaptively adjusting the particle velocity and position update rules. Meanwhile, the chaotic perturbation strategy is used to jump out of the local optimal solution and achieve the efficient search of the global optimal solution. The MSC-PSO algorithm has a unique multi-strategy fusion mechanism and chaotic disturbance characteristics, which can dynamically adjust the inventory and classification of power grid materials, thereby optimizing the warehousing system. The multi-strategy chaos mechanism refers to introducing multiple chaotic mapping strategies such as Logistic and Tent into the population initialization and search disturbance process, and improving the solution space coverage through multi mapping synergy to avoid premature convergence. This mechanism mixes different chaotic sequences to enable particles to obtain adaptive perturbation amplitudes at different stages, enhancing search diversity and the ability to escape local optima. The dynamic adjustment module structure of the MSC-PSO algorithm for power grid material inventory is shown in Fig. 1.

In Fig. 1, the dynamic adjustment module of power grid material inventory consists of three parts: data integration layer, intelligent optimization core layer, and execution feedback layer. The data integration layer collects various key parameters in real-time through Internet of Things sensors, enterprise management systems, and historical operation and maintenance data, and integrates external environmental parameters (such as meteorological disaster warning, regional load fluctuations) to construct input data packets. The formula for calculating safety stock is denoted in Eq. (1)[20].

$$S_s = \alpha \cdot \sigma \cdot \sqrt{L} \tag{1}$$

In Eq. (1), S_s means the safety stock level. α represents the safety stock factor (determined by the importance of materials, such as 95% service level corresponding to $\alpha = 1.65$). σ means the standard deviation of demand.L means the procurement lead time (constant value). By quantifying inventory buffer, it can cope with demand fluctuations and supply chain delays. The optimization core layer first uses Tent chaotic mapping to initialize the particle swarm, uniformly covering the solution space such as replenishment cycle, safety stock threshold, and economic batch size. The calculation formula for chaotic sequence values is shown in Eq. (2)[21].

$$y_{k+1} = \beta \cdot \min(y_k, 1 - y_k) \tag{2}$$

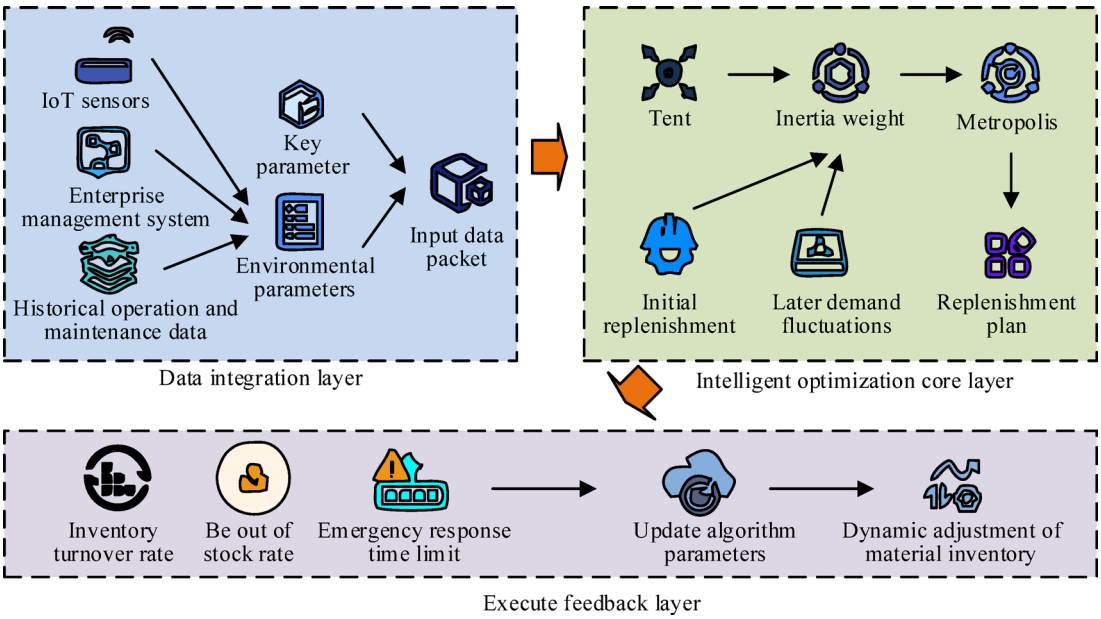

Fig. 1. Dynamic adjustment module for power grid material inventory.

In Eq. (2), y_{k+1} means the chaotic sequence value of the $k+1$th iteration. y_k represents the chaotic sequence value of the k th iteration. β represents the chaotic parameter (usually taken as β to ensure traversal). The calculation formula for Tent chaotic mapping is shown in Eq. (3)[22].

$$Y_{Tent} = \begin{cases} \frac{y_k}{d}, & 0 \leqslant y_k < d \\ \frac{1-y_k}{1-d}, & d \leqslant y_k \leqslant 1 \end{cases} \tag{3}$$

In Eq. (3), Y_{Tent} represents the result of Tent chaotic mapping. d represents a constant with a value range of $0 < d < 1$. Studying the generation of uniformly distributed initial solutions through Tent chaotic mapping can avoid particle swarm aggregation in local areas. Then, global exploration and local development are balanced through adaptive inertia weight. The calculation method of inertia weight is shown in Eq. (4)[23].

$$w_k = w\max - \frac{\left(w\max - w_{\min}\right) \cdot k}{K\max} \tag{4}$$

In Eq. (4), w_k represents the inertia weight of the k th iteration. $w\max = 0.9$ means the upper limit of weight. $w_{\min} = 0.4$ means the lower limit of weight. $K\max$ represents the maximum number of iterations. In the initial stage, the focus is on global optimization of multi-level warehouse collaborative replenishment strategies, while in the later stage, the emphasis is on matching demand fluctuations. The Metropolis criterion, which simulates the annealing mechanism, is also introduced to accept the suboptimal solution with probability and circumvent the local optimal trap due to the coupling of regional inventories. The acceptance probability of the Metropolis criterion is calculated as shown in Eq. (5)[24].

$$P_{Metropolis} = \begin{cases} 1, & \text{if } \Delta f \leqslant 0 \\ \exp\left(-\frac{\Delta f}{k_{Bo} \cdot T_{now}}\right), & \text{if } \Delta f > 0 \end{cases} \tag{5}$$

In Eq. (5), $P_{Metropolis}$ means the probability of accepting a new solution. Δf represents the difference between the objective function of the new solution and the current solution. k_{Bo} stands for Boltzmann constant, used to control the scale of acceptance probability. T_{now} represents the current temperature parameter and reflects the search stage of the algorithm. The initial temperature is high and gradually decreases with iteration. The optimization results are analyzed using Pareto front analysis to generate a multi-objective replenishment plan (such as minimizing inventory costs and stockout risks), which automatically triggers supplier orders through blockchain smart contracts. The weight method transforms a multi-objective problem into a single objective problem by assigning weights to each objective function. The formula for calculating the comprehensive objective function is denoted in Eq. (6)[25].

$$F(x) = \sum_{i=1}^{n} \widetilde{w}_i \cdot f_i(x) \tag{6}$$

In Eq. (6), $F(x)$ represents the comprehensive objective function. $\widetilde{w}_i$ represents the weight of the i th objective function. $f_i(x)$ is the value of the i th objective function. The execution layer has a built-in dynamic allocation network that adjusts delivery priorities in real-time based on inventory saturation and demand urgency. The execution feedback layer updates the algorithm parameter library through reverse iteration by monitoring indicators such as inventory turnover rate, stockout rate, and emergency response timeliness, for example, adjusting the safety stock weight coefficient based on historical stockout events. The formula for updating the algorithm parameter library is shown in Eq. (7)[26].

$$\alpha_{\text{new}} = \alpha_{\text{old}} + \gamma \cdot (S_{\text{actual}} - S_{\text{threshold}}) \tag{7}$$

In Eq. (7), α_{new} represents the updated algorithm parameter library. α_{old} represents the algorithm parameter library before the update. γ represents learning rate (dynamically adjusting step size). S_{actual} represents the statistical value of historical stockout events. $S_{\text{threshold}}$ represents the out-of-stock tolerance threshold. This method can dynamically optimize the safety stock factor based on actual stockout feedback. The calculation formula for inventory turnover rate is shown in Eq. (8)[27].

$$R_{\text{turnover}} = \frac{\text{COGS}}{\frac{1}{2}(I_{\text{initial}} + I_{\text{final}})} \tag{8}$$

In Eq. (8), R_{turnover} represents inventory turnover rate. COGS represents the cost of material outflow. I_{initial} and I_{final} represent the initial and final inventory levels, respectively. This module also provides geographic information system visualization dashboards, real-time mapping of regional inventory heat maps, transfer path topologies, and warning signals (such as transformer inventory in a warehouse below a safety threshold), supporting dynamic intervention by management personnel. The structure of the intelligent classification module for power grid materials using the MSC-PSO algorithm is shown in Fig. 2.

As shown in Fig. 2, the intelligent classification module for power grid materials is a multidimensional dynamic classification system based on a chaotic weight matrix. The data preprocessing part integrates multi-source information such as material attribute data (value, specifications), operation and maintenance data (failure

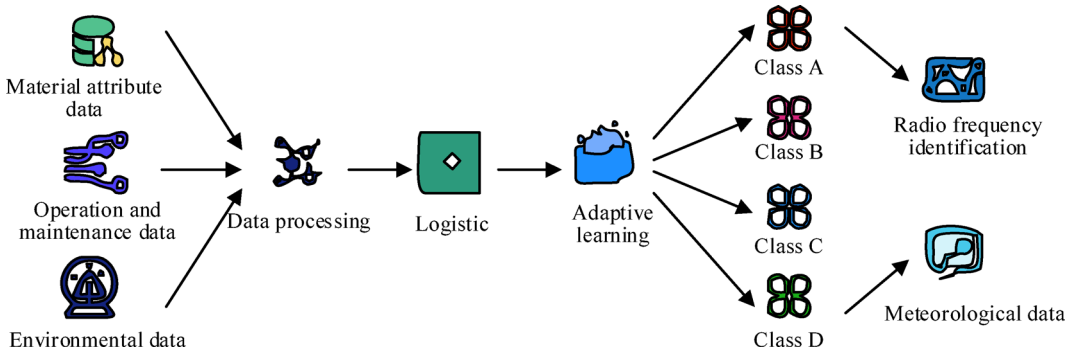

Fig. 2. Structure of intelligent classification module for power grid materials.

rate, replacement frequency), environmental data (regional disaster risk), etc., cleans outliers through fuzzy logic algorithms, and extracts demand periodic features using time series analysis. The intelligent classification engine adopts the chaos disturbance strategy in the MSC-PSO algorithm. Firstly, a random weight sequence within the (0, 1) interval is generated through Logistic chaotic mapping, and the calculation formula is denoted in Eq. (9)[28].

$$Z_{k+1} = \lambda \cdot Z_k \cdot (1 - Z_k) \tag{9}$$

In Eq. (9), Z_{k+1} represents the chaotic state value of the $k+1$th iteration. Z_k represents the chaotic state value of the k th iteration. λ represents chaos control parameters. The calculation formula for constructing a multidimensional classification matrix (covering multiple dimensions such as cost, emergency level, and demand volatility) is shown in Eq. (10).

$$M_{m,n} = \sum_{d=1}^{D} \omega_d^{(k)} \cdot f_d(S_{m,n}) \tag{10}$$

In Eq. (10), $M_{m,n}$ means the comprehensive rating matrix of material m in the n th classification dimension. $\omega_d^{(k)}$ represents the dynamic weight of the d th dimensional feature (generated by chaotic mapping). $f_d(S_{m,n})$ represents the dth dimensional feature normalization function (Min-Max normalization). This matrix can quantify the classification priority of materials in a multidimensional feature space. Next, based on adaptive learning factors, it dynamically adjusts the classification threshold, such as increasing the emergency weight coefficients of insulators and repair tools during typhoon season. The calculation formula for the adaptive learning factor is shown in Eq. (11).

$$\delta_k = \delta_{\min} + (\delta_{\max} - \delta_{\min}) \cdot e^{-\eta \cdot k} \tag{11}$$

In Eq. (11), δ_k means the learning factor of the k th iteration. $\delta_{\max}$ and $\delta_{\max}$ represent the max and mini values of the adaptive learning factor, respectively. η represents the attenuation coefficient, which is used to control the learning rate and adjust the amplitude. e represents natural logarithm. The materials are dynamically classified into four categories: Class A refers to high-value and high stress acute materials, such as transformers; Class B refers to medium turnover and medium risk materials, such as cables; Class C refers to low value and conventional materials, such as screw consumables; Class D refers to uncertain demand materials, such as ice melting devices. Class A materials are tracked in real-time using radio frequency identification technology and dynamic safety stock is set up. Class D materials are linked with the data interface of the meteorological department to trigger a pre-procurement agreement. The module also has a built-in self-learning mechanism, which optimizes the chaotic weight matrix in reverse through classification accuracy to enhance the classification robustness in disaster scenarios. The process of optimizing the storage of power grid materials using the MSC-PSO algorithm is shown in Fig. 3.

As shown in Fig. 3, the MSC-PSO algorithm first integrates multi-source data and extracts features, and then generates an initial particle swarm based on Tent chaotic mapping. Each particle represents a combination of replenishment cycle, safety stock threshold, and economic batch strategy to cover the global solution space. The fitness function integrates multi-objective weights and dynamically adjusts the evaluation criteria based on the disaster level. The algorithm balances global exploration and local optimization through adaptive inertia weights, and introduces the Metropolis criterion to accept suboptimal solutions and avoid local optima. The Pareto front solution set generated iteratively is filtered and triggers automatic replenishment of smart contracts. Finally, the parameters are updated in reverse based on actual data to enhance the dynamic adaptability of the strategy. To ensure the efficiency of subsequent material transportation and reduce the sorting time of goods in the warehouse, a fishbone storage layout design was adopted. The layout of fishbone type storage shelves for power grid materials is shown in Fig. 4.

As shown in Fig. 4, the V-shaped main channel extends from the central storage area to both sides to form a fishbone spine, with parallel branch channels distributed on both sides. Class A high-value materials (such as

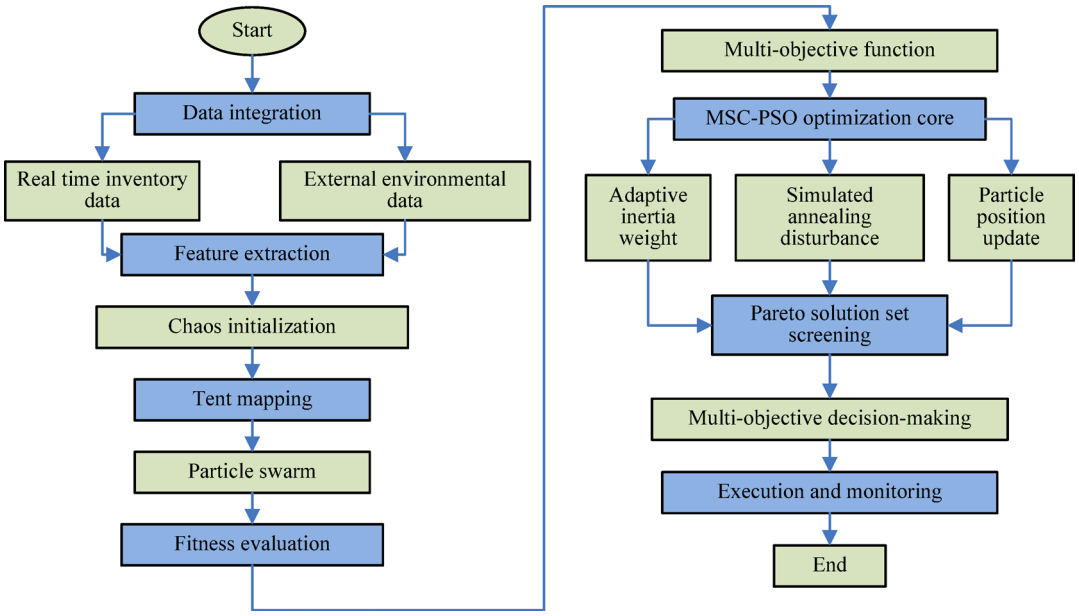

Fig. 3. Process of MSC-PSO algorithm for optimizing storage of power grid materials.

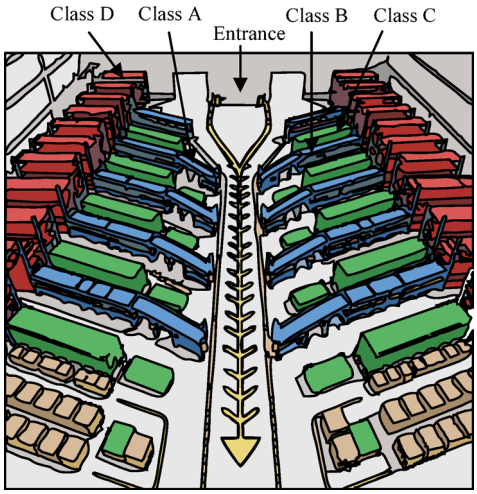

Fig. 4. Fishbone type storage layout of power grid materials.

transformers) are located adjacent to both sides of the main channel, Class B medium frequency materials (such as cable stacks) are located in the proximal branch channel, Class C consumables (such as hardware boxes) are placed on remote through shelves, and Class D emergency materials (such as ice melting devices) are stored in the end movable shelf area. This layout can shorten the distance of material picking and walking, while also facilitating dynamic adjustment of stored materials. The pseudocode of the MSC-PSO algorithm is shown below.

Distribution path planning of power grid material supply chain based on IICA

The MSC-PSO algorithm, as a multi-strategy fusion adaptive chaotic PSO algorithm, achieves dynamic adjustment and classification of power grid material inventory through adaptive strategies and chaotic disturbance strategies. The fishbone storage layout method is helpful for the rapid sorting of goods. The warehouse coordinates, material allocation ratios, and node demand information output by the first stage warehouse optimization module will serve as inputs and constraints for the second stage IICA path planning, used to initialize the distribution network structure and path search space. This ensures that path planning operates under the constraints of warehouse layout, achieving dynamic collaboration and coupling optimization between warehousing and distribution processes. To improve the efficiency of subsequent power grid material supply chain distribution and reduce transportation costs, the IICA was adopted to plan the distribution path of power grid material supply chain. To improve the performance of the IICA, an immune cost function was introduced to integrate the path cost of material distribution, emergency response priority, and inventory

```
Input:
   MaxIter         // Maximum number of iterations
   N               // Population size (500)
   w_max, w_min    // Inertial weight upper and lower bounds
   pm              // Chaos disturbance probability (0.05)
   F(x)            // Multi objective fitness function (cost, time, energy consumption, etc.)
Output:
   Pareto_Set      // Final non dominated solution set

1: Initialize population X = {x1, x2, ⋯ , xN} by chaotic mapping
2: Initialize velocities V randomly
3: Evaluate fitness F(xi) and record personal best pbest and global best gbest
4: for t = 1 to MaxIter do
5:    Update inertia weight:
        w = w_max - (w_max - w_min) * (t / MaxIter)
6:    for each particle xi do
7:       Update velocity:
           vi = w * vi + c1 * rand() * (pbest_i - xi)
                + c2 * rand() * (gbest - xi)
8:       Update position:
           xi = xi + vi
9:       With probability pm apply chaotic perturbation:
           if rand() < pm then
              xi = Chaos(xi)
           end if
10:      Apply immune selection to maintain diversity:
           xi = ImmuneSelect(xi, Pareto_Set)
11:   end for
12:   Evaluate fitness F(xi)
13:   Update pbest and Pareto_Set via non-dominated sorting
14:   Update gbest based on Pareto dominance and crowding distance
15: end for

16: return Pareto_Set
```

MSC-PSO Algorithm.

constraints into a multi-objective optimization function[29]. This function can suppress premature convergence of the algorithm by dynamically adjusting the antibody concentration threshold. The structure of the immune cost function is shown in Fig. 5.

As shown in Fig. 5, the immune cost function constructs a multi-objective optimization framework by integrating path cost, emergency response priority, and inventory constraints. Immune penalty correction is a constraint correction strategy based on immune cloning theory, which applies adaptive penalty factors to candidate solutions that do not meet the constraints through antigen recognition and antibody affinity evaluation. This mechanism automatically weakens the competitiveness of infeasible solutions during the search process and enhances the search density in the vicinity of feasible solutions, thereby improving the algorithm's constraint handling ability and feasible domain convergence speed. The path cost integrates transportation distance, fuel consumption, and fixed vehicle costs to form a basic economic indicator. The emergency response adopts an exponential time window penalty function to quantify the urgency of delayed delivery of materials. Inventory constraints are dynamically adjusted for storage capacity deviations through an over capacity penalty mechanism. On this basis, the immune mechanism introduced by the immune cost function can enhance the global optimization ability. The immune cost function utilizes the information entropy of antibody similarity to evaluate population diversity, combined with a dynamically decaying concentration threshold to suppress high concentration antibody reproduction and prevent premature convergence. Among them, the concentration threshold gradually decreases with the increase of iteration times, allowing moderate convergence in the initial stage and strengthening diversity preservation in the later stage. The problem of transforming multi-objective optimization into maximizing a composite cost function is studied by adaptively balancing path economy, emergency timeliness and inventory stability through dynamic weighting coefficients, and immunizing the cost function. Under the framework of the IICA, this mechanism is embedded in the assimilation and competition stages to drive antibody cloning, mutation, and population updates, ultimately achieving efficient search for

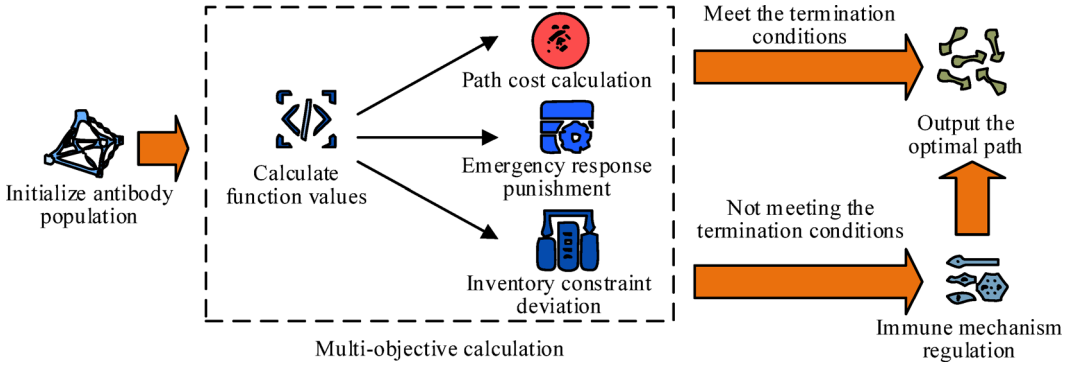

Fig. 5. Structure of immune cost function.

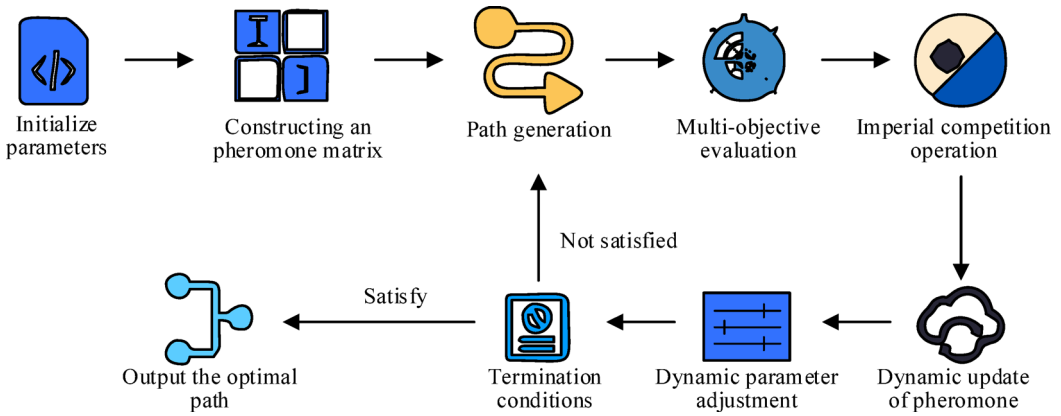

Fig. 6. Structure of path optimization module.

the global optimal delivery path. The algorithm also integrates ACO to form a material distribution path optimization module. The structure of the path optimization module is indicated in Fig. 6.

In Fig. 6, the flowchart of the material distribution path optimization module begins with network parameter initialization, covering distribution nodes, vehicle capacity, and emergency rule configuration. Subsequently, a dynamic pheromone matrix is constructed to map path cost, inventory constraints, and emergency priority to the search gradient of ant colony algorithm. The calculation formula for pheromone is shown in Eq. (12)[30].

$$\varsigma_{xy}(t) = \varsigma_{xy}(t-1) \cdot (1-\psi) + \Delta\varsigma_{xy}^{elite} \tag{12}$$

In Eq. (12), $\varsigma_{xy}(t)$ represents the pheromone concentration of path (x, y) at time t, indicating the historical optimization accumulation of this path. ψ represents the volatility coefficient of pheromones $(0 < \psi < 1)$, which controls the decay rate of historical pheromones. Its initial value is small to maintain diversity, and it increases later to accelerate convergence. $\Delta\varsigma_{xy}^{elite}$ represents the pheromone increment of elite path to path (x, y), and the calculation formula is denoted in Eq. (13).

$$\Delta\varsigma_{xy}^{\text{elite}} = \frac{\kappa}{\text{Cost}_{\text{best}}} \tag{13}$$

In Eq. (13), κ represents the pheromone intensity constant. $\text{Cost}_{\text{best}}$ represents the comprehensive value of the optimal path. The path generation stage simulates the heuristic behavior of ants, performs path segment crossover and pheromone guided mutation operations within the framework of imperial competition, and dynamically generates candidate delivery solutions. Each 'ant' represents a colony, and the formula for calculating the probability of path selection is denoted in Eq. (14).

$$P_{xy}^{k'} = \frac{[\varsigma_{xy}(t)]^{\vartheta} \cdot [\theta_{xy}]^{\Gamma}}{\sum_{z \in \mathcal{A}_{num}} [\varsigma_{xz}(t)]^{\vartheta} \cdot [\theta_{xz}]^{\Gamma}} \tag{14}$$

In Eq. (14), $P_{xy}^{k'}$ represents the probability of the k' th ant choosing path (x, y) from node x, which is determined by both the pheromone and heuristic functions. θ_{xy} stands for heuristic function, usually taking the reciprocal of the path ($\theta_{xy} = \frac{1}{d_{xy}}$), representing the natural attraction of the path (x, y) (such as higher attraction with shorter distance). ϑ represents the pheromone factor (with a range of values), which controls the weight of pheromone concentration. The larger the value, the stronger the path dependence on historical experience. Γ represents the heuristic factor (with a range of values), which controls the weight of the heuristic function. If the value is too large, it can easily fall into local optima. $\mathcal{A}_{num}$ represents the set of nodes currently accessible to Ant num, initially consisting of all unvisited nodes, and dynamically updated along the path. The multi-objective evaluation module can also call the immune cost function to quantify transportation economy, inventory stability, and emergency timeliness indicators, combined with Pareto front screening and antibody concentration monitoring mechanisms to avoid local optimal traps. The heuristic function θ_{xy} can be extended to a multi-objective function, such as combining transportation costs, inventory deviation, and emergency timeliness. The calculation formula is shown in Eq. (15).

$$\theta_{xy} = \omega_1 \cdot d_{xy} + \omega_2 \cdot \mathrm{InvPenalty} + \omega_3 \cdot \mathrm{EmergDelay} \tag{15}$$

In Eq. (15), $\mathrm{InvPenalty}$represents the penalty cost for inventory deviation. $\mathrm{EmergDelay}$ stands for emergency delivery delay penalty. ω_1, ω_2, and ω_3 represent corresponding weights, which are adaptively adjusted by Pareto front. The pheromone update process is based on the elite empire path to strengthen the concentration of pheromones in the critical path, and balances global exploration and local development through adaptive volatility coefficient. The pheromone adaptive balancing mechanism dynamically adjusts the weight ratio of PSO global information and IICA competitive information by constructing an pheromone update function based on performance differences. This mechanism enhances the exploration ability in the early stage of search and improves the utilization depth in the later stage of convergence, achieving an adaptive balance of global local search intensity, thereby improving the overall stability and convergence efficiency of the hybrid algorithm. The algorithm periodically adjusts the target weights and the size of the empire cluster, and ultimately outputs the optimal path for power grid material supply chain distribution when meeting the convergence threshold or resource constraints. The MSC-PSO-IICA model was constructed by integrating the above-mentioned warehouse optimization and path optimization methods. The structure of the MSC-PSO-IICA model is denoted in Fig. 7.

As shown in Fig. 7, the MSC-PSO-IICA model is an intelligent optimization framework that integrates multiple strategies and achieves global optimization of power grid material warehousing and distribution through a hierarchical collaborative mechanism. The data integration layer collects real-time warehouse data (inventory levels, demand fluctuations) and path parameters (distribution nodes, vehicle capacity), and integrates external environmental information such as meteorological warnings. The preprocessing of data adopts fuzzy logic to clean outliers and extract periodic demand features from time series. In the warehouse optimization module of the MSC-PSO algorithm, a multi-population adaptive collaborative strategy is studied, using Tent chaotic mapping to generate uniformly distributed initial solutions to cover the solution space, and dynamically balancing global search (such as cross warehouse allocation) and local development (safety stock matching) through adaptive inertia weights. The Metropolis criterion, which introduces simulated annealing mechanism, accepts suboptimal solutions to avoid local optima caused by regional inventory coupling. The optimization results are filtered by Pareto front and trigger automatic replenishment of blockchain smart contracts. The warehouse goods are arranged in a fishbone structure to shorten the movement time of goods inside the warehouse. In the path planning module of the IICA, the immune cost function is used to integrate path cost, emergency response priority, and inventory constraints. The antibody concentration threshold is used to dynamically suppress premature convergence, and the dynamic pheromone matrix of the ant colony algorithm is combined to guide path search. Then the pheromone accumulation of the critical path is reinforced by the elite empire path. The storage optimization module and path planning module achieve two-way data linkage through a collaborative feedback layer. Warehouse inventory status updates the inventory constraints

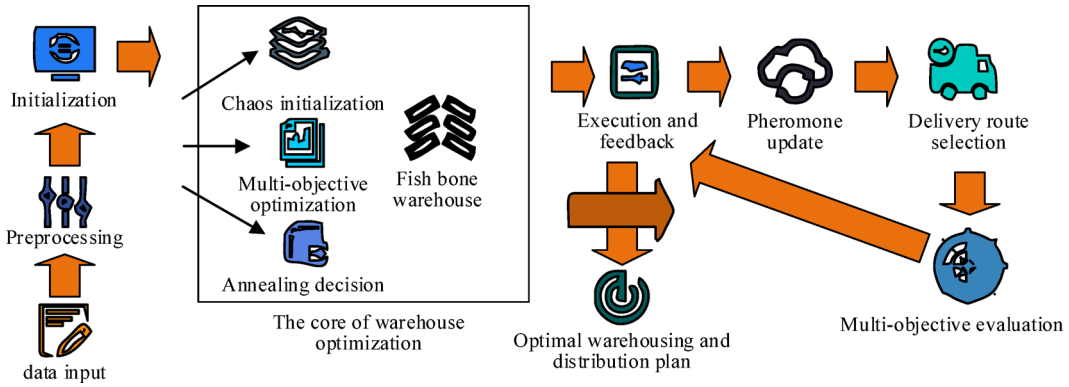

Fig. 7. Structure of MSC-PSO-IICA model.

```
Input:
   N            // population size
   MaxIter      // maximum iterations
   w_max, w_min  // inertia weight bounds
   c1, c2       // acceleration coefficients
   pm           // chaos perturbation probability
Output:
   Updated particle positions and velocities

1: Initialize particles Xi and velocities Vi
2: Evaluate fitness F(Xi) and record pbest and gbest
3: for t = 1 to MaxIter do
4:     Compute adaptive inertia weight:
          w = w_max - (w_max - w_min) * (t / MaxIter)
5:     for each particle Xi do
6:         Update velocity:
              Vi = w * Vi + c1 * rand() * (pbest_i - Xi)
                   + c2 * rand() * (gbest - Xi)
7:         Update position:
              Xi = Xi + Vi
8:         if rand() < pm then
9:             Xi = ChaosMap(Xi)     // chaotic perturbation
10:        end if
11:    end for
12:    Re-evaluate F(Xi) and update pbest and gbest
13: end for

14: return Xi, Vi
```

Adaptive PSO Mechanism.

of path planning in real time, while the distribution results inversely optimize the safety inventory parameters. MSC-PSO-IICA helps to reduce the cost of warehousing and improve the efficiency of material distribution in emergency situations through chaotic perturbation, immune mechanism and multi-objective collaborative strategy.

This article proposes a dynamic inertia weight and chaotic disturbance collaborative adjustment strategy based on the intensity of disaster scene disturbances in adaptive PSO, which achieves an adaptive balance between global exploration and local convergence in search. In the immune ICA module, this article constructs a path correction mechanism that combines immune memory and dynamic antibody selection, significantly enhancing the stability and path recovery ability of the algorithm under disaster uncertainty. The pseudocode for adaptive PSO and immune ICA is as follows.

Result

Performance analysis of MSC-PSO algorithm

A high-performance experimental platform was established to assess the performance of the MSC-PSO algorithm. The CPU of the experimental platform was Intel i5-13600KF, the GPU was NVDIA GeForce RTX 4070 Ti, the memory was 32GB DDR4 3200 MHz, and the hard drive was 1 TB PCIE 3.0. The software environment was based on Ubuntu 22.04 system, integrating Python 3.10 development environment (NumPy, Pandas, PyTorch library), Arduino IDE embedded development tool, and Gazebo simulation platform. Real time performance monitoring was achieved through Prometheus + Grafana, and a zero cost open source development ecosystem was built using VS Code and Git to meet the parallel computing needs of MSC-PSO algorithm with a particle size of 500. To ensure the stability of the algorithm, the main parameter values were based on the empirical settings of typical swarm intelligence algorithms. At the same time, ablation experiments were conducted to verify the rationality of the selected parameter settings, as shown in Table 1.

According to Table 1, under the original parameter combination of inertia weight (0.9 – 0.4), mutation probability of 0.05, and population size of 500, the algorithm achieved optimal performance in terms of convergence iteration times, delivery cost, and solution time. The input parameters of MSC-PSO algorithm are denoted in Table 2.

```
Input:
   Empires          // set of empires in ICA
   MaxIter
   β               // assimilation coefficient
   ImmuneRate       // probability of immune correction
Output:
   Updated empire states and solutions

1: Initialize empires and colonies
2: Evaluate fitness and identify imperialists
3: for t = 1 to MaxIter do
4:     for each empire e do
5:         Assimilation of colonies:
               Colony = Colony + β * rand() * (Imperialist - Colony)
6:         Revolution (random exploration):
               Colony = Revolution(Colony)
7:         if rand() < ImmuneRate then
8:             Colony = ImmuneCorrection(Colony)
               // immune memory selects historical elite solutions
9:         end if
10:        Update empire power and compare colony with imperialist
11:    end for
12:    Imperialistic competition among empires
13: end for

14: return Updated Empires
```

Immune-Enhanced ICA Mechanism.

Test ID	Inertial weight (max, min)	Mutation probability (pm)	Population size	Average solution time (s)	Average delivery cost ($)
A1	0.9,0.4	0.05	500	1.17	23,451
A2	0.9,0.6	0.05	500	1.35	23,890
A3	0.8,0.4	0.05	500	1.22	23,580
B1	0.9,0.4	0.01	500	1.20	23,510
B2	0.9,0.4	0.10	500	1.40	23,950
C1	0.9,0.4	0.05	100	0.60	24,500
C2	0.9,0.4	0.05	300	0.85	23,720
C3	0.9,0.4	0.05	700	1.60	23,480

Table 1. Results of MSC-PSO optimal parameter ablation experiment.

The dataset used the Grid Supply Chain dataset, which includes 100 suppliers and 500 delivery points. This dataset was chosen because it covers all kinds of key data of grid material supply, such as the demand, inventory, transport cost, emergency response priority and other information of different materials, and also contains a variety of grid material supply scenarios, which can comprehensively and comprehensively assess the performance of the MSC-PSO algorithm. The comparative algorithm adopted Constrained Particle Swarm Optimization-based Model Predictive Control (CPSO-MPC) algorithm and Particle Swarm Optimization Back Propagation Artificial Neural Network (PSO-BP-ANN) algorithm[31,32]. The optimal storage solution time and computational resource utilization of each algorithm are shown in Fig. 8.

According to Fig. 8 (a), the MSC-PSO algorithm had the shortest average solution time (1.17s), significantly better than the CPSO-MPC algorithm (2.28s) and PSO-BP-ANN algorithm (2.98s). The time curve tended to stabilize with the increase of iteration times, indicating that the algorithm has fast convergence speed and high stability. The PSO-BP-ANN algorithm had a higher computational complexity due to the fusion of neural network backpropagation mechanism, resulting in a longer solution time than the MSC-PSO algorithm.

Parameter name	Description	Typical range/Example
Inertia weight	Dynamically adjusted weight balancing global and local search	0.4 to 0.9
Acceleration coefficients	Weights for individual and social experience in velocity update	1.5 to 2.0
Swarm size	Number of particles for parallel search	30 to 500
Max iterations	Termination condition balancing computation and precision	50 to 200
Dimensions	Number of variables to optimize (e.g., control or inventory parameters)	3 or higher
Chaotic mapping	Generates uniform initial solutions to avoid particle clustering	0.5
Pareto threshold	Fitness tolerance for selecting non-dominated solutions	0.1 to 0.5
Annealing temperature	Controls suboptimal solution acceptance with initial temperature and decay	Initial 100, decay 0.95
Collaborative weight	Dynamic coupling weight between inventory and routing planning	0.3 to 1.0

Table 2. Input parameters of MSC-PSO algorithm.

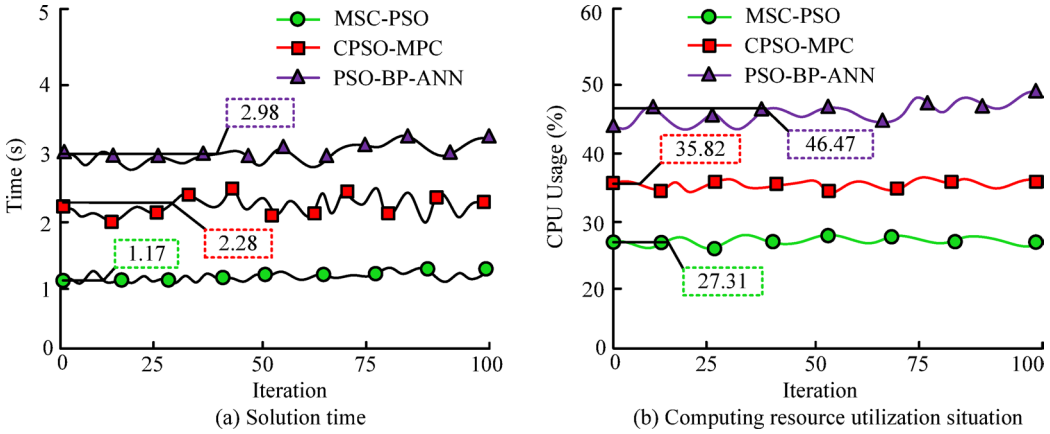

Fig. 8. Comparison of optimal storage solution time and computing resource utilization for various algorithms.

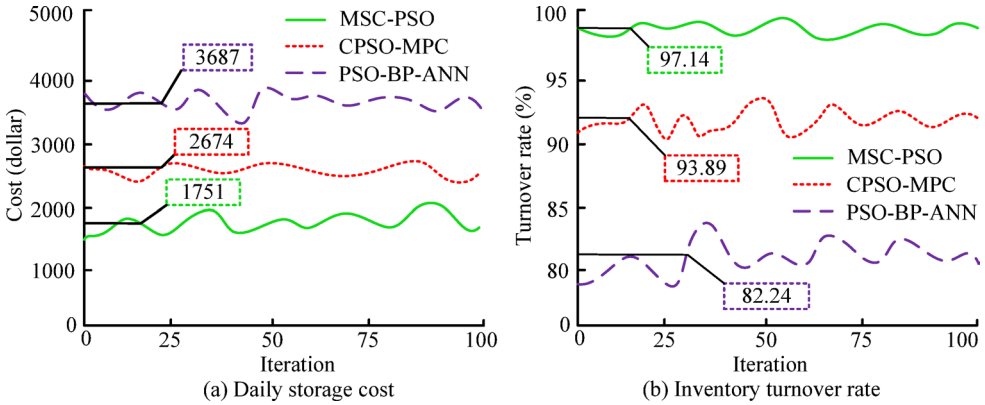

Fig. 9. Comparison of optimized warehousing costs and inventory turnover rates using different algorithms.

According to Fig. 8 (b), the MSC-PSO algorithm had the lowest average CPU rate (27.31%) and the highest resource utilization efficiency. Its usage curve fluctuated smoothly, indicating that the algorithm has good hardware load control. The PSO-BP-ANN algorithm had a CPU usage rate of up to 46.47% due to synchronous updates of multi-layer network parameters, far exceeding other algorithms. The CPSO-MPC algorithm had the second highest occupancy rate (35.82%), which is related to the structural complexity of its model predictive control. MSC-PSO can achieve the best balance between solving efficiency and resource consumption through algorithm structure optimization, and is suitable for industrial scenarios with high real-time requirements and limited hardware resources. The optimized warehousing costs and inventory turnover rates using different algorithms are shown in Fig. 9.

According to Fig. 9 (a), the optimized MSC-PSO algorithm had the lowest warehousing cost, with an average daily cost of $1751, which was 52.51% lower than the PSO-BP-ANN algorithm ($3687). In Fig. 9 (b), the optimization effect of the algorithm on inventory turnover was positively correlated with its cost control capability. The MSC-PSO algorithm had the highest turnover rate, with an average turnover rate of 97.14%, which was 3.25% points higher than the CPSO-MPC algorithm (about 93.89%). The PSO-BP-ANN algorithm had the lowest turnover rate of 82.24%, reflecting its inadequate adaptability to demand fluctuations in replenishment strategies. The adaptive inertia weight measurement of MSC-PSO algorithm can effectively balance cost control and turnover improvement, avoiding premature convergence to suboptimal solutions. The MSC-PSO algorithm could reduce warehousing costs and improve inventory turnover to cope with various unexpected situations. The MSC-PSO algorithm also combined a fishbone warehouse structure to improve the efficiency of dynamic adjustment of goods in the warehouse. To verify the performance of MSC-PSO algorithm in multi-objective and uncertain scenarios, a comparative experiment was conducted with Nondominated Sorting Genetic Algorithm II (NSGA-II) and Multi-objective Evolutionary Algorithm Based on Decomposition (MOEA/D) on the same dataset and termination conditions. The comparison indicators included Pareto coverage, Hypervolume (HV), average delivery cost, average solution time, convergence algebra, and cost volatility. The results are shown in Table 3.

According to Table 3, the Pareto coverage and HV of MSC-PSO were significantly higher, indicating that it can find a wider and better set of non dominated solutions among cost time energy consumption objectives. The average delivery cost and variance of MSC-PSO were the lowest, indicating that the algorithm can not only find low-cost solutions, but also had better operational stability. In contrast, NSGA-II performed the worst in terms of cost fluctuations and convergence speed, indicating that it is prone to premature convergence or slow convergence under the constraint coupling and uncertain disturbances of this problem. From the perspective of computational efficiency, MSC-PSO also had advantages in convergence algebra and average solution time, indicating that the proposed adaptive weights and multi-strategy perturbations accelerate the convergence process without significantly increasing computational overhead. Statistical tests show that MSC-PSO has statistically significant advantages in key indicators (HV, average cost) ($p < 0.05$), supporting its superiority over the two typical multi-objective algorithms in the simulation scenario presented in this paper. Overall, the experiment has verified the effectiveness, stability, and scalability of MSC-PSO in multi-objective and uncertain emergency logistics scheduling problems. To demonstrate the efficiency improvement of cargo adjustment in fishbone warehouse structure, a comparison was made between the traditional rectangular warehouse cargo arrangement and the fishbone warehouse cargo arrangement in terms of cargo access frequency. The comparison results are shown in Fig. 10.

From Fig. 10 (a), the traditional rectangular warehouse goods arrangement method had no obvious regularity in the frequency of goods access and retrieval. This indicated that the storage location of goods was not effectively matched with the frequency of use, and high-frequency goods were not concentrated in convenient areas, resulting in frequent crossing of handling equipment across different areas and limited overall access efficiency. As shown in Fig. 10 (b), high-frequency goods were concentrated on both sides of the main channel (such as near the V-shaped spine), while low-frequency goods were stored on the remote branch shelves, forming a gradient distribution of "high-frequency concentration and low-frequency dispersion". The combination of fish bone warehouse cargo arrangement method and cargo classification method can significantly shorten the average handling distance of high-frequency goods.

Analysis of the practical application effect of MSC-PSO-IICA model

The MSC-PSO algorithm could quickly obtain the optimal solution for warehouse adjustment by dynamically adjusting and optimizing the layout of goods, which not only reduced warehousing costs but also improved handling efficiency. To verify the practical application effect of the MSC-PSO-IICA model, actual tests were conducted in a certain power grid material warehouse. The accuracy of the MSC-PSO-IICA model for classifying different types of materials and the average transportation time within the warehouse are shown in Fig. 11.

According to Fig. 11 (a), the MSC-PSO-IICA model achieved classification accuracies of 98.73%, 96.58%, 94.12%, and 91.45% for Classes A, B, C, and D materials, respectively, all higher than CPSO-MPC and PSO-BP-ANN. Its advantage lies in the precise identification of high-frequency material priorities and dynamic weight adaptation through multi-strategy collaborative optimization. According to Fig. 11 (b), the average transportation time for Class A material under the MSC-PSO-IICA model was only 12.45 s, which is 18.79%

Indicator	MSC-PSO	NSGA-II	MOEA/D
Pareto coverage rate (%)	96.78 ± 1.15	89.12 ± 2.30	91.45 ± 1.88
HV	0.842 ± 0.009	0.776 ± 0.018	0.803 ± 0.014
Average delivery cost ($)	23,451 ± 310	26,780 ± 870	25,500 ± 620
Average solution time (s/time)	1.17 ± 0.06	2.05 ± 0.12	1.62 ± 0.09
Convergent Algebra	45 ± 4	78 ± 7	60 ± 5
Cost standard deviation ($)	310	870	620

Table 3. Performance comparison of MSC-PSO with NSGA-II and MOEA/D (30 independent operation results, Mean ± Standard Deviation). Note: All algorithms were independently run 30 times under the same evaluation function and random seed strategy; Using a two sample *t*-test on HV and average cost, MSC-PSO showed significant differences compared to the two control methods at $p < 0.05$.

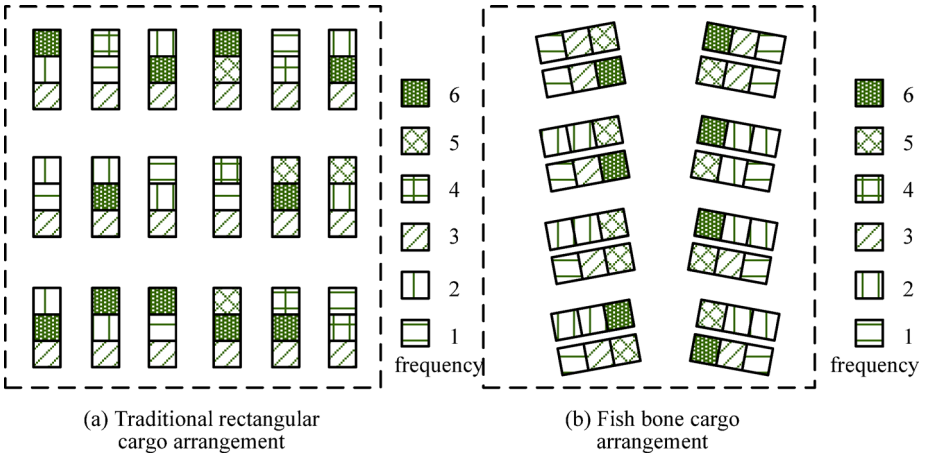

Fig. 10. Comparison of goods access frequency between rectangular warehouse layout and fishbone warehouse layout.

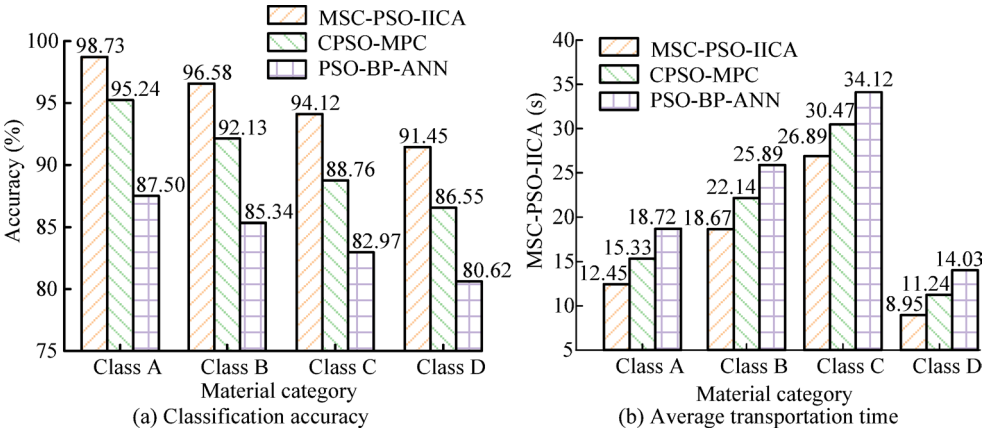

Fig. 11. Comparison of material classification accuracy and in-warehouse average transportation time among different algorithms.

less than CPSO-MPC (15.33 s), thanks to the collaborative design of path optimization and fishbone layout. From this, the MSC-PSO-IICA model achieves a dual breakthrough of high-precision classification and efficient transportation through a joint optimization mechanism of classification and transportation. To improve the transparency and reproducibility of the experiment, this study built a test scenario based on the emergency logistics dispatching records of a provincial power grid in recent three years, including four types of emergencies, namely typhoon, earthquake, mountain fire and rainstorm. Each algorithm ran under the same node layout, the same number of vehicles, and consistent capacity constraints, and adopted a unified parameter upper limit and termination condition. To avoid accidental effects, all results were based on the average of 30 times independent runs and had a stable trend. Delivery cost and delivery time were core evaluation indicators that reflect the overall resource scheduling efficiency and response speed, respectively, and could comprehensively measure the scheduling performance of the algorithm under emergency conditions. The distribution costs and delivery times of the MSC-PSO-IICA model in response to different types of emergencies in the power grid material supply chain are shown in Table 4.

According to Table 4, MSC-PSO-IICA showed significant advantages in distribution cost and response time over the comparison algorithm in four types of emergencies (typhoon, earthquake, mountain fire and rainstorm). By conducting a two sample *t*-test on the results of 30 independent runs, the comparison algorithm with "*" significantly outperformed MSC-PSO-IICA under the condition of $p < 0.05$, indicating that its performance improvement is statistically significant and not caused by random fluctuations. In typhoon scenarios, the delivery cost of MSC-PSO-IICA was $23,451, which is $4443 lower than CPSO-MPC ($27894) and $8706 lower than PSO-BP-ANN ($32157). The delivery time was also reduced by 2.22 h and 4.34 h respectively, indicating that the model can achieve better route planning under frequent wind and disaster conditions. In earthquake scenarios, MSC-PSO-IICA controlled the delivery time to 5.67 h, which is 2.22 h faster than CPSO-MPC, and the cost was significantly lower, indicating that the algorithm has stronger adaptability to road congestion and changes in warehouse accessibility caused by earthquakes. In the mountain fire and rainstorm scenarios, the

Type of emergency	Algorithm	Delivery cost (dollar)	Delivery time (h)
Typhoon	MSC-PSO-IICA	23,451	4.56
	CPSO-MPC	27,894*	6.78*
	PSO-BP-ANN	32,157*	8.90*
Earthquake	MSC-PSO-IICA	25,671	5.67
	CPSO-MPC	30,121*	7.89*
	PSO-BP-ANN	35,672*	9.87*
Wildfire	MSC-PSO-IICA	20,341	3.45
	CPSO-MPC	24,563*	5.60*
	PSO-BP-ANN	29,781*	7.65*
Heavy Rain	MSC-PSO-IICA	19,895	3.21
	CPSO-MPC	23,451*	5.32*
	PSO-BP-ANN	28,562*	7.43*

Table 4. Distribution costs and delivery times of power grid material supply chain. Note: Values with "*" indicate significant difference ($p < 0.05$) compared to the results of MSC-PSO-IICA over multiple runs.

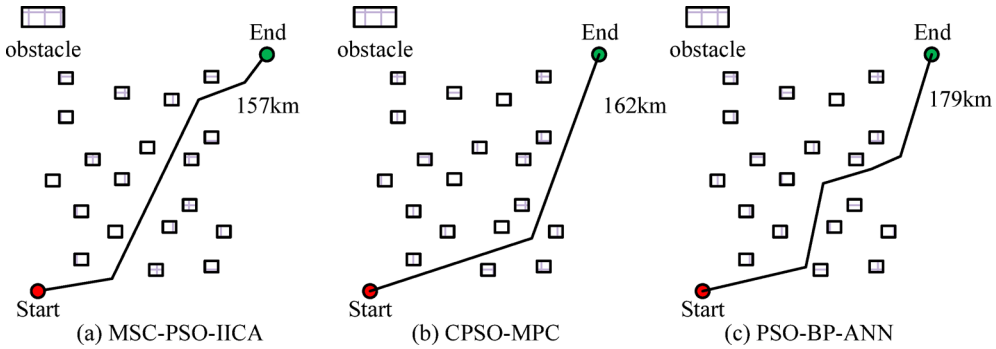

Fig. 12. Optimal supply chain distribution paths planned by different algorithms in earthquake scenarios.

method also obtained the lowest distribution cost and the shortest response time. The cost of the rainstorm scenario (US $19895) was US $8667 lower than that of PSO-BP-ANN, and the time was 4.22 h lower, reflecting the robustness of the algorithm under continuous dynamic disturbance. Further analysis of Table 4 reveals that MSC-PSO-IICA not only dominates on average, but also maintains a stable performance improvement trend in different disaster scenarios without significant fluctuations. This robustness stems from the two-stage collaborative mechanism of the model structure: the adaptive chaotic search in the first stage can quickly identify effective warehouse layouts in disaster scenarios, reducing overall delivery mileage from the source. The second stage of immune IICA improves the adaptability of path planning to disaster disturbances through dynamic deviation correction, thereby maintaining fast convergence in complex environments. In contrast, CPSO-MPC and PSO-BP-ANN exhibited more significant performance fluctuations when disaster intensity changes, further verifying the reliability, robustness, and generalization ability of MSC-PSO-IICA in uncertain environments. Taking earthquake scenarios as an example, the optimal distribution path of the supply chain planned by various methods is shown in Fig. 12.

According to Fig. 12 (a), the total length of the earthquake scene distribution path planned by the MSC-PSO-IICA model was 157 km, with smooth and coherent path trajectories and no redundant turns, indicating its excellent global obstacle avoidance ability. As shown in Fig. 12 (b), the total length of the CPSO-MPC algorithm path was 162 km. Although it avoided all obstacles, it increased redundant distance to reduce turning, resulting in a longer delivery path. As shown in Fig. 12 (c), the PSO-BP-ANN model had a total path length of 179 km, with multiple jagged turns in the end region of the trajectory, and some sections were too close to obstacles, posing a safety hazard. The immune cost function of the PSO-BP-ANN model ensured the minimum distance between obstacles and vehicles by introducing path smoothness and safety distance penalty terms. The fused ant colony algorithm could quickly converge to the shortest path in complex terrain, reducing path redundancy. It can be seen that the MSC-PSO-IICA model, with its multi-strategy collaborative optimization, can plan the supply chain distribution path with the least number of obstacle detours and the smoothest trajectory in sudden disaster scenarios. In other aspects, the actual application effects of the MSC-PSO-IICA model are denoted in Table 5.

According to Table 5, the MSC-PSO-IICA model demonstrated comprehensive optimization capabilities in smart grid logistics scenarios. In terms of multi-objective optimization, the Pareto front coverage rate reached 96.78%, indicating that it has almost global coverage in the dual objective balance optimization of cost and carbon emissions. The path planning capability led with a dynamic adjustment success rate of 98.24%, which

Parameter category	Parameter name	Value	Application scenario
Multi-objective optimization	Pareto front coverage (%)	96.78	Multi-objective balance (cost & carbon emissions) optimization
Path planning	Dynamic path adjustment success rate (%)	98.24	Real-time obstacle avoidance in typhoon scenarios (GIS + LSTM integration)
Inventory management	Inventory turnover rate improvement (%)	32.15	Smart replenishment strategy for B/C-class supplies
Energy consumption optimization	Transportation energy reduction (%)	22.73	Multi-modal energy synergy optimization (truck-drone collaboration)
Computational efficiency	Single iteration time (seconds)	0.45	Solving efficiency for logistics optimization problems
Solution quality	Global optimum deviation (Std. Dev.)	0.08	Solution stability in complex multimodal scenarios
Emergency response	Material mismatch rate (%)	1.23	Precise matching of D-class emergency supplies (with RFID verification)
Algorithm robustness	High-dimensional convergence success rate (%)	89.12	Global convergence in 500-dimensional node optimization

Table 5. Actual application effect of MSC-PSO-IICA model.

can efficiently avoid collapsed road sections in typhoon scenarios. Inventory management was jointly modeled through classification coding and demand forecasting, resulting in a 32.15% increase in turnover rate for Class B and Class C materials. In terms of energy consumption optimization, the multimodal transport collaborative control model reduced transportation energy consumption by 22.73%. In terms of computational efficiency, solving the optimal path for supply chain distribution in a single iteration only took 0.45 s. Combined with the stability advantage of the global optimal solution deviation degree (0.08), the algorithm's efficient convergence ability has been verified. The emergency response and robustness performance were equally outstanding, with a mismatch rate of only 1.23% for Class D materials and a convergence success rate of 89.12% for 500 dimensional node optimization. In summary, MSC-PSO-IICA has achieved industry-leading levels in efficiency, energy consumption, stability, and emergency response through multi-strategy collaborative design, providing reliable technical support for the refinement, dynamism, and low-carbon development of smart grid logistics.

Discussion

The MSC-PSO-IICA method proposed in this study outperforms traditional PSO, immune computing, and neural network optimization methods in various types of emergency event scenarios. However, these numerical results themselves cannot fully reflect the management value and engineering applicability of the model in actual power grid emergency logistics scenarios. Therefore, this section conducts in-depth discussions on operational management insights, trade-offs between computation and scalability, model interpretability and implementation costs, potential risks and limitations, and future development directions, in response to the scientific and mature requirements of algorithm deployment in complex supply chain scenarios.

From the perspective of management and operation, the experimental results show that MSC-PSO-IICA can maintain stable low-cost and short-term advantages under conditions of significant changes in disaster intensity. Its significance lies not only in numerical optimization itself, but also in supporting the emergency decision-making process of power grid enterprises. The two-stage structure of the model corresponds to the dual decision-making mechanism of "warehouse preparation path scheduling" in the actual emergency process of enterprises. Therefore, its performance differences in different disaster scenarios can provide enterprises with more refined stocking strategies, more reliable emergency material distribution suggestions, and more responsive path selection schemes. In addition, the warehouse layout and allocation results output by the model can assist managers in identifying key warehouse nodes and sensitive distribution paths, which helps to establish a more robust regional backup system.

In terms of balancing computational efficiency, model scalability, and adaptability, the advantage of MSC-PSO-IICA mainly lies in its dynamic adaptability to unexpected events, but there is also a certain resource overhead. Compared to single metaheuristic algorithms, hybrid structures bring stronger global local search complementarity, but also increase the synchronization cost between iterations. Therefore, when the node size rapidly expands or the scheduling frequency significantly increases, the computational cost of the model will increase accordingly, and it is necessary to determine the appropriate group size and update strategy based on task requirements. In addition, for more complex constraint scenarios such as high-dimensional disaster disturbances, cross regional distribution, and time window constraints, although the current structure can be adapted through parameter adjustments, its scalability still relies on deeper structural optimization.

In terms of interpretability and implementation cost, although the results of MSC-PSO-IICA can provide intuitive path and cost output, the search logic and immune enhancement mechanism of the intermediate process are difficult to fully explain to non-technical personnel. This may increase communication costs and technical dependencies in algorithm deployment. In addition, the model needs to continuously update warehouse data, disaster information, and real-time traffic. In practical applications, there are problems such as inconsistent data interfaces, missing data, or insufficient real-time performance, which bring additional costs to model maintenance.

Regarding potential risks and limitations, there are still several points that need to be pointed out in this study: (1) When the scale of the problem expands, the number of constraints increases, or real-time optimization is required, high-frequency decision-making scenarios may not fully meet real-time requirements. (2) The model performs well under specific supply chain structures and parameter settings, but its scalability is limited when migrating across industries or scenarios. (3) The model obtains a solution set through a complex interactive search process, and its interpretability still needs further enhancement.

In response to the above limitations, future research can be conducted in the following directions: (1) Research should be conducted on lightweight hybrid optimization framework to reduce computational burden. At the same time, it should explore the implementation methods based on distributed computing or edge computing, so that the algorithm has better real-time response capability. (2) An adaptive parameter adjustment mechanism is constructed, and transfer learning and metaheuristic scheduling strategies are explored to improve cross-domain scalability and robustness. (3) An interpretable optimization framework is introduced, such as rule-based extraction, sensitivity analysis, and evolution path visualization, to provide decision-making basis for algorithm output.

Overall, although MSC-PSO-IICA has demonstrated significant advantages in experiments, its true scientific value lies in providing an emergency supply chain scheduling framework that can integrate multi strategy optimization features. By further simplifying the model, enriching application scenarios, and improving interpretability, this model is expected to have higher application value in the field of power grid and even broader emergency logistics.

Conclusion

This study aimed to solve the problems of high cost, low resource utilization, and slow emergency response in the storage and supply chain distribution of power grid materials. It proposed an optimization method for power grid material storage based on MSC-PSO algorithm and a supply chain distribution path planning method based on IICA, and constructed the MSC-PSO-IICA model. The MSC-PSO algorithm effectively balanced global search and local convergence speed through multi-strategy fusion, and used chaotic disturbances to jump out of local optimal solutions, achieving dynamic adjustment and classification optimization of power grid material inventory. The findings denoted that the algorithm had the shortest average solution time of 1.17s, the lowest average CPU rate of 27.31%, and the optimized average daily storage cost was $1751, which is 52.51% lower than the PSO-BP-ANN algorithm. The average inventory turnover rate was 97.14%, which was 3.25% points higher than the CPSO-MPC algorithm. When dealing with typhoon, earthquake, fire, rainstorm and other emergencies, the MSC-PSO-IICA model was significantly better than the comparison algorithm in terms of distribution cost and time. For example, in a typhoon scenario, the delivery cost of the MSC-PSO-IICA model was $23,451, which was $4443 and $8706 less than CPSO-MPC and PSO-BP-ANN, respectively. The delivery time was 4.56 h, which is 2.22 h and 4.34 h shorter than the two models. The MSC-PSO-IICA model can reduce the storage and transportation costs of power grid materials and improve transportation efficiency. However, the accuracy of the MSC-PSO-IICA model is limited by the quality of historical data. In the future, blockchain smart contracts will be used to achieve data interoperability across the entire supply chain from suppliers-warehousing-distribution, further compressing the supply chain response cycle.

Data availability

The datasets used and/or analyzed during the current study available from the corresponding author on reasonable request.

Received: 5 September 2025; Accepted: 17 December 2025
Published online: 22 December 2025

References

1. Ari, I. A low carbon pathway for the turkish electricity generation sector. *GLCE* **1** (3), pp147–153 (2023). https://doi.org/10.47852/bonviewGLCE3202552
2. Wang, S. et al. Future demand for electricity generation materials under different climate mitigation scenarios. *Joule* **7** (2), 309–332 (2023). https://doi.org/10.5281/zenodo.7023703
3. Konde, A. L., Kusaf, M. & Dagbasi, M. An effective design method for grid-connected solar PV power plants for power supply reliability. *Energy Sustain. Dev.* **70** (1), 301–313. https://doi.org/10.1016/j.esd.2022.08.006 (2022).
4. Solyali, D., Safaei, B., Zargar, O. & Aytac, G. A comprehensive state-of-the-art review of electrochemical battery storage systems for power grids. *Int. J. Energy Res.* **46** (13), 17786–17812. https://doi.org/10.1002/er.8451 (2022).
5. Chen, Z., Kleijn, R. & Lin, H. X. Metal requirements for Building electrical grid systems of global wind power and utility-scale solar photovoltaic until 2050. *Environ. Sci. Technol.* **57** (2), 1080–1091. https://doi.org/10.1021/acs.est.2c06496 (2022).
6. Rouholamini, M. et al. A review of modeling, management, and applications of grid-connected Li-ion battery storage systems. *IEEE Trans. Smart Grid*. **13** (6), 4505–4524. https://doi.org/10.1109/TSG.2022.3188598 (2022).
7. Han, J. et al. Hydrogen-powered smart grid resilience. *Energy Convers. Econ.* **4** (2), 89–104. https://doi.org/10.1049/enc2.12083 (2023).
8. Peng, P. et al. Cost and potential of metal-organic frameworks for hydrogen back-up power supply. *Nat. Energy*. **7** (5), 448–458 (2022). https://doi.org/10.1038/s41560-022-01013-w
9. Peng, L., Wang, L. & Wang, S. Hybrid arithmetic optimization algorithm for a new multi-warehouse joint replenishment and delivery problem under trade credit. *Neural Comput. Appl.* **35** (10), 7561–7580. https://doi.org/10.1007/s00521-022-08052-0 (2023).
10. Hu, X. & Chuang, Y. F. E-commerce warehouse layout optimization: systematic layout planning using a genetic algorithm. *Electron. Commer. Res.* **23** (1), 97–114. https://doi.org/10.1007/s10660-021-09521-9 (2023).
11. Das, J. N., Tiwari, M. K., Sinha, A. K. & Khanzode, V. Integrated warehouse assignment and carton configuration optimization using deep clustering-based evolutionary algorithms. *Expert Syst. Appl.* **212** (1), 118680–118681. https://doi.org/10.1016/j.eswa.2022.118680 (2023).
12. Wang, Y., Roy, N. & Zhang, B. Multi-objective transportation route optimization for hazardous materials based on GIS,J. Loss prev. *Process. Ind.* **81** (1), 104954–104955. https://doi.org/10.1016/j.jlp.2022.104954 (2023).
13. Hu, X. et al. Optimization and implementation strategy for low-carbon multimodal transport routes: A collaborative approach between government and transport enterprises. *J. Clean. Prod.* **502** (1), 145341–145342. https://doi.org/10.1016/j.jclepro.2025.145341 (2025).
14. Mahat, D., Niranjan, K., Naidu, C. S., Babu, S. B. T. & Kumar, M. S. AI-driven optimization of supply chain and logistics in mechanical engineering. *Proc. IEEE UPCON*, **10**(1), 1611–1616, (2023). https://doi.org/10.1109/UPCON59197.2023.10434905

15. Pham, V. H. S., Nguyen, V. N. & Nguyen Dang, N. T. Hybrid Whale optimization algorithm for enhanced routing of limited capacity vehicles in supply chain management. *Sci. Rep.* **14** (1), 793–794. https://doi.org/10.1038/s41598-024-51359-2 (2024).
16. Qezelbash-Chamak, J., Badamchizadeh, S. & Seifi, A. A fast-response mathematical programming approach for delivering disaster relief goods: an earthquake case study. *Transp. Lett.* **16** (9), 1091–1114. https://doi.org/10.1080/19427867.2023.2270238 (2024).
17. Corso, M. P. et al. Evaluation of visible contamination on power grid insulators using convolutional neural networks, *Electr. Eng* **105** (6), 3881–3894. https://doi.org/10.1007/s00202-023-01915-2 (2023).
18. Sharma, D. K. et al. A review on smart grid telecommunication system. *Mater. Today Proc.* **51(**1), 470–474 (2022). https://doi.org/10.1016/j.matpr.2021.05.581
19. Schäfer, B. et al. Understanding braess' paradox in power grids,Nat. *Commun* **13** (1), 5396–5397. https://doi.org/10.1038/s41467-022-32917-6 (2022).
20. Tiwari, S. & Kumar, A. Advances and bibliographic analysis of particle swarm optimization applications in electrical power system: concepts and variants,Evol. *Intell* **16** (1), 23–47. https://doi.org/10.1007/s12065-021-00661-3 (2023).
21. Zhang, J. & Ye, J. Reactive power optimization based on tent-chebyshev switching mapping particle swarm optimization. *Proc. IEEE EEPS*. **1** (1), 420–424 (2024). https://doi.org/10.1109/EEPS63402.2024.10804317
22. Xu, Z. & Hu, C. Chaotic adaptive particle swarm algorithm based on tent mapping for multi-objective optimization of combined cooling, heating, and power source-store-load systems. *Proc. SPIE ISAEECE.* **12704(1)**, 851–856 (2023). https://doi.org/10.1117/12.2680521
23. Li, T. et al. Multi-objective operation optimization of microgrid source-grid-load-storage based on tent mapping improved snake optimization algorithm. *Proc. IEEE ICCEPE*. **1** (1), 429–433 (2024). https://doi.org/10.1109/ICCEPE62686.2024.10931665
24. Khou, S. A., Olamaei, J. & Hosseini, M. H. Strategic scheduling of the electric vehicle-based microgrids under the enhanced particle swarm optimization algorithm. *Sci. Rep.* **14** (1), 30795–30796. https://doi.org/10.1038/s41598-024-81049-y (2024).
25. Sharma, S. & Kumar, V. A comprehensive review on multi-objective optimization techniques: Past, present and future. *Arch. Comput. Methods Eng.* **29**, 5605–5633. https://doi.org/10.1007/s11831-022-09778-9 (2022).
26. Shi, H., Gao, Z., Fang, L., Zhai, J. & Sun, H. Research on inventory control method based on demand response of power big data. *Scalable Comput. Pract. Exp.* **25** (3), 1781–1789. https://doi.org/10.12694/scpe.v25i3.2695 (2024).
27. Wang, B., Zhang, P., He, Y., Wang, X. & Zhang, X. Scenario-oriented hybrid particle swarm optimization algorithm for robust economic dispatch of power system with wind power. *J. Syst. Eng. Electron.* **33** (5), 1143–1150. https://doi.org/10.23919/JSEE.2022.000110 (2022).
28. Aydın, M. S. & Çam, E. Application of chaotic maps to economic load dispatch problem,Karadeniz Fen bilim. *Derg* **14** (3), 1630–1639. https://doi.org/10.31466/kfbd.1530071 (2024).
29. Blackwell, A. D. The ecoimmunology of health and disease: the hygiene hypothesis and plasticity in human immune function. *Annu. Rev. Anthropol.* **51** (1), 401–418. https://doi.org/10.1146/annurev-anthro-101819-110236 (2022).
30. Quque, M. et al. Eusociality is linked to caste-specific differences in metabolism, immune system, and somatic maintenance-related processes. *Ant Species Cell. Mol. Life Sci.* **79** (1), 29–30. https://doi.org/10.1007/s00018-021-04024-0 (2022).
31. Gbadega, P. A. & Sun, Y. A hybrid constrained particle swarm optimization-model predictive control (CPSO-MPC) algorithm for storage energy management optimization problem in micro-grid. *Energy Rep.* **8**, 692–708 (2022). https://doi.org/10.1016/j.egyr.2022.10.035
32. Zhang, J., Chen, C., Wu, C., Kou, X. & Xue, Z. Storage quality prediction of winter jujube based on particle swarm optimization-backpropagation-artificial neural network (PSO-BP-ANN). *Sci. Hortic.* **331** (1), 112789 (2024). https://doi.org/10.1016/j.scienta.2023.112789

Author contributions

J.P.G., T.W. and K.R.H. processed the numerical attribute linear programming of communication big data, and the mutual information feature quantity of communication big data numerical attribute was extracted by the cloud extended distributed feature fitting method. J.G.W., J.C.W. and J.W. Combined with fuzzy C-means clustering and linear regression analysis, the statistical analysis of big data numerical attribute feature information was carried out, and the associated attribute sample set of communication big data numerical attribute cloud grid distribution was constructed. J.P.G. and J.F.W. did the experiments, recorded data, and created manuscripts. All authors read and approved the final manuscript.

Declarations

Competing interests

The authors declare no competing interests.

Ethical statement

The authors declare that this research is original and has not been published previously. No part of the manuscript involves plagiarism, duplicate submission, data fabrication, data falsification, or any form of academic misconduct. All data sources, algorithms, and referenced materials used in this study have been properly cited, and the research was conducted in accordance with recognized academic and ethical standards. The authors take full responsibility for the integrity and accuracy of the content presented in this work.

Additional information

Correspondence and requests for materials should be addressed to J.G.